

The enhancement in density is greatest in the intermediate-mfp regime [Fig. 5(b)] as predicted by the theory. In Fig. 5(b) the magnitude of the density jump decreases with each additional mirror. According to Eq. (2), the measured increases in n_1 as the number of cells is increased corresponds to a confinement time τ scaling as L^2 for the first three cells, relaxing to L as more cells are added. This is to be expected in the presence of recombination loss and radial loss, which becomes more important as the confinement time due to multiple-mirror action increases. The ratio of n_1 with five mirror cells (n_{\max}) to n_1 with one mirror cell (n_{\min}) is plotted as a dash-dotted curve in Fig. 4. It is seen to follow generally the values of τ_z .

*Research sponsored by the National Science Foundation under Grant No. GK-27538, and by the U. S. Air Force Office of Scientific Research under Grant No. AF-AFOSR-69-1754. One of the authors (B.G.L.) held a U. S. Atomic Energy Commission Fellowship.

¹B. Grant Logan, A. J. Lichtenberg, M. A. Lieberman, and A. Makhijani, *Phys. Rev. Lett.* **28**, 144 (1972).

²B. Grant Logan, Fourth Quarterly Progress Report on Plasma Research, Electronics Research Laboratory, University of California, Berkeley, 1969 (unpublished).

³G. I. Budker, V. A. Mirnov, and D. D. Ryutov, *Pis'ma Zh. Eksp. Teor. Fiz.* **14**, 320 (1971) [*JETP Lett.* **14**, 212 (1971)].

⁴A. Makhijani, Second Semiannual Progress Report on Plasma Research, Electronics Research Laboratory, University of California, Berkeley, 1971 (unpublished).

Parametric Instability and Anomalous Heating Due to Electromagnetic Waves in Plasma*

M. Porkolab, V. Arunasalam, and R. A. Ellis, Jr.

Plasma Physics Laboratory, Princeton University, Princeton, New Jersey 08540

(Received 28 September 1972)

Experimental results are presented which verify the fundamental aspects of the parametric instability of whistler waves. The accompanying fast heating of plasma is interpreted to be due to anomalous absorption.

In this Letter we present experimental results which show (i) the parametric decay of a large-amplitude electron cyclotron wave (whistler) and/or an electron plasma wave in a plasma in a magnetic field; and (ii) the associated anomalous heating of both electrons and ions. In addition, the decay spectrum and the heating were measured as the incident microwave power, the pulse duration, and the magnetic field strength were varied. Although recently predicted by theory,¹⁻³ to our knowledge, this is the first time that the parametric decay and associated plasma heating due to whistler waves have been measured in laboratory experiments.

The experiments were carried out in the 3-m-long Princeton L-3 linear device. The plasma was produced in the steady state by a 5-cm-diam, 20-cm-long helical slow wave structure,⁴ which injected up to 1 kW S-band microwave power into a magnetic mirror configuration. In the present experiments $f_0 = 2.45$ GHz, $f_{ce} = 2.45$ to 5.0 GHz, $f_{pe} \geq 10$ GHz, so that $f_0 \leq f_{ce} < f_{pe}$ (where f_{ce} and f_{pe} are the electron cyclotron and the electron

plasma frequencies, respectively). Recently Lisitano, Fontanesi, and Bernabei proposed that such structures heat the plasma nonresonantly by excitation and collisional absorption of electron waves.⁵ However, in our device we find that such nonresonant plasma sources operate in two modes; (1) at low pressures (i.e., $p \leq 10^{-3}$ Torr in He gas) and low densities ($n_0 \leq 2 \times 10^{12}$ cm⁻³), long-wavelength ($\lambda_{\parallel} \approx 3$ to 10 cm, $\lambda_{\perp} \approx 5$ cm) electron plasma waves are excited which obey the dispersion relation

$$1 = \omega_{pe}^2 \cos^2 \theta / \omega^2 + \omega_{pe}^2 \sin^2 \theta / (\omega^2 - \omega_{ce}^2), \quad (1)$$

where $\cos \theta = k_{\parallel} / k$, $\sin \theta = k_{\perp} / k$, and $k_{\parallel} = \vec{k} \cdot \vec{B} / B$. These waves decay parametrically into short-wavelength electron plasma waves [also satisfying Eq. (1)] and ion acoustic waves which propagate at an angle to the external magnetic field. These results are in agreement with recent theoretical predictions.^{1,2} (2) At higher pressures ($p \geq 2 \times 10^{-3}$ Torr in He gas) and higher densities ($n_0 \geq 3 \times 10^{12}$ to 10^{13} cm⁻³) whistler waves with wavelengths $\lambda_{\parallel} = 0.7$ to 2.5 cm, $\lambda_{\perp} \approx 5$ cm are

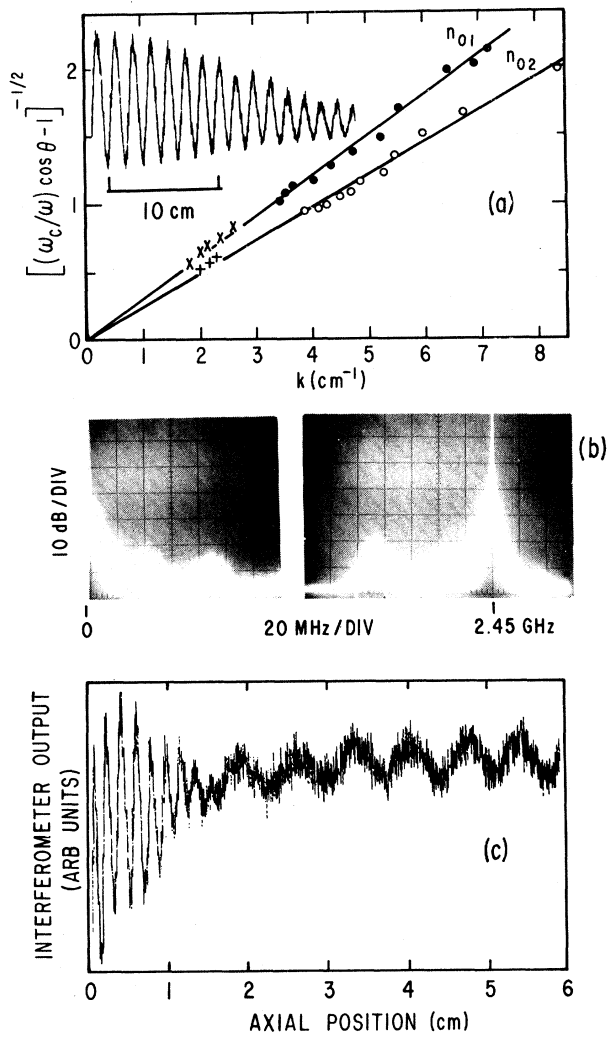


FIG. 1. (a) Experimental verification of the whistler wave dispersion relation [Eq. (2)]. The dots are associated with the rf source at 2.45 GHz. The crosses represent linearly propagated waves at 1 GHz. $n_{01} = 3.5 \times 10^{12}$, $n_{02} = 6.5 \times 10^{12}$ cm⁻³. (b) Typical decay spectrum in cw operation. $P_{in} \approx 0.8$ kW. (c) Interferometer output showing the ion acoustic waves at 7.5 MHz; $f_0/f_{ce} = 0.67$.

excited. These waves satisfy the following dispersion relation:

$$c^2 k^2 / \omega^2 = 1 - \omega_{pe}^2 / \omega(\omega - \omega_{ce} \cos \theta), \quad (2)$$

where $k^2 = k_{\parallel}^2 + k_{\perp}^2$. These waves are observed to decay by two different processes, both of which have been recently predicted theoretically¹⁻³: (a) Decay into a second whistler wave and an ion acoustic wave occurs due to mode-mode coupling by the $\vec{j} \times \vec{E}_w$ forces of the waves.³ The wavelengths are such that the usual selection

rules³ are obeyed for $k_s = -k_0$ and $k_A = 2k_0$ [where $\omega_s(k_s)$, the sideband, is another whistler and $\omega_A(k_A)$ is the ion acoustic wave]. (b) The other process consists of parametric decay into a short-wavelength ion acoustic wave and an electron plasma wave such that $k_s = -k_A$, and $k_A \gg k_0$.^{1,2} In this case the parametric coupling of the decay waves is due to the electric field of the pump wave. The decay waves propagate at an angle to the external magnetic field. For the sake of brevity, we present here only the experimental results obtained in the high-density regime, i.e., the decay of whistler waves. The results obtained for the decay of electron plasma waves were qualitatively similar, and will be presented in a later publication.

A typical interferometer output showing the whistler wave propagation in the uniform magnetic field region is presented in the inset in Fig. 1. We have not yet made a study of the damping of the wave. Figure 1(a) shows a direct verification of the linear dispersion relation of whistler waves, including finite values of k_{\perp} . The solid lines are the theoretical curves. In Fig. 1(b) we show a typical decay spectrum as obtained from an rf probe 50 cm from the plasma source. In order to identify the decay processes, we have measured both the low-frequency waves (ω) and the high-frequency sideband waves, $\omega_0 - \omega$. This was done by passing through tunable narrow-band-pass filters ($\Delta f/f \approx 3\%$) located between the interferometer and the rf probes. A typical interferometer output of the acoustic waves at 7.5 MHz is shown in Fig. 1(c). Note the existence of two different wavelengths, i.e., $\lambda_{\parallel} \approx 2$ mm and $\lambda_{\parallel} \approx 0.8$ cm. The reference probe is located at $z = 0$. The perpendicular wavelengths have also been measured, and were found to be standing waves, with a mixture of components of $\lambda_{\perp} \approx 1.8$ mm, and $\lambda_{\perp} \approx 2$ cm. The smaller value of λ_{\perp} is believed to be associated with the $\lambda_{\parallel} = 2$ mm component. In particular, since in the present case $v_A = 10^6$ cm/sec (He gas with temperature of $T_e = 5$ eV), the linear ion acoustic-wave dispersion relation ($\omega = kv_A$) is satisfied. Furthermore, the sideband waves (i.e., $f_0 - 7.5$ MHz) consisted of a mixture of short-wavelength waves (i.e., $\lambda_{\parallel} = 2$ mm) and longer wavelengths ($\lambda_{\parallel} \approx 1.6$ cm), the latter being the same as the pump wavelength. Thus, we see that the short-wavelength waves are due to parametric coupling of ion acoustic waves and electron plasma waves [i.e., the measured values of k_{\parallel} and k_{\perp} satisfied Eq. (1)]. On the other hand, the longer-wavelength compo-

nents are associated with $\vec{j} \times \vec{E}_w$ coupling of two whistlers (with $k_s = -k_0$) with an ion wave with $k_A = 2k_0$. In particular, by varying the magnetic field, we verified that the longer-wavelength ion wave always satisfied the relation $k_A = 2k_0$.

From our measurements we see that the longer-wavelength ion waves do not satisfy the linear dispersion relation. This we believe to be due to the broadening of resonant frequencies by the finite pump wave amplitude (i.e., in these measurements B_w was considerably above threshold). In particular, the measurement of waves at other frequencies showed a band of frequencies with nearly the same values of k_{\parallel} , but with slightly different values of k_{\perp} . Similar effects have also been observed in the case of parametric decay into the shorter-wavelength waves. In the latter case a numerical analysis of the parametric dispersion relation² showed that in the case of the pump considerably above threshold, a band of frequencies may be unstable with essentially the same k_{\parallel} (the most unstable one), but with slightly different values of k_{\perp} . Similarly, in the case of the $\vec{j} \times \vec{E}_w$ type of decay a two-dimensional theory may be necessary to explain the observed spread of frequencies above threshold. Alternatively, a nonlinear theory may be necessary for a complete description of the ob-

served broad frequency spectrum.

In order to study the heating of the plasma due to these instabilities, we installed a second slow wave structure, at the opposite end of the device from the plasma source. By applying a fast rise-time ($t = 50$ nsec) microwave pulse at 2.30 GHz, with the pulse width varied from 0.5 to 10 μ sec, we observed strong heating of both the electrons and the ions. The incident microwave power could be varied in the range 0 to 6 kW. The decay spectrum at the sidebands was monitored by sweeping the spectrum analyzer externally. In these experiments the cw plasma source was operated at relatively low powers (300 W). In Fig. 2 we show a typical saturated power spectrum as a function of incident power. We see that the low-frequency components ($f \approx 5$ MHz) have very low thresholds, and grow 5 orders in magnitude before saturating. The higher-frequency components (which are associated with shorter wavelengths), have much higher thresholds and saturate at lower amplitudes. This is presumably due to the strong Landau damping of these modes.

The thresholds for the decay have been determined from the transmitted power levels. The threshold fields obtained were in reasonable agreement with theoretical estimates (within a factor of 2 to 3). So far we have made comparisons only with the one-dimensional mode-mode coupling theory,³ and with the two-dimensional parametric theory.^{1,2} In particular, the $\vec{j} \times \vec{E}_w$ type decay has very low thresholds (a few tens of watts, i.e., $B_w/B_0 \approx 10^{-4}$).

In Figs. 3(a) and 3(b) we show the electron and the ion distribution functions, as determined from time-resolved retarding potential energy analyzer measurements. We found that the main body temperatures remained cold (i.e., $\Delta T/T \lesssim 50\%$ as determined from pulsed Langmuir probe measurements). On the other hand, the tails of both the electron and the ion distribution functions were heated by 1 to 2 orders of magnitude. In particular, for $P_{in} = 6$ kW, 10- μ sec-long pulses, $T_e = 100$ to 150 eV, $T_i = 10$ to 20 eV. The number of electrons and ions that were heated amounted to approximately 10% of the total number of either species. Thus, approximately 10% of the energy went directly into heating ions. The heating time of the electrons was 1–2 μ sec, whereas that of the ions was 5–10 μ sec. At high powers nearly complete absorption was observed, and the energy deposit accounted for the observed heating. Additional experiments in which the pulse length

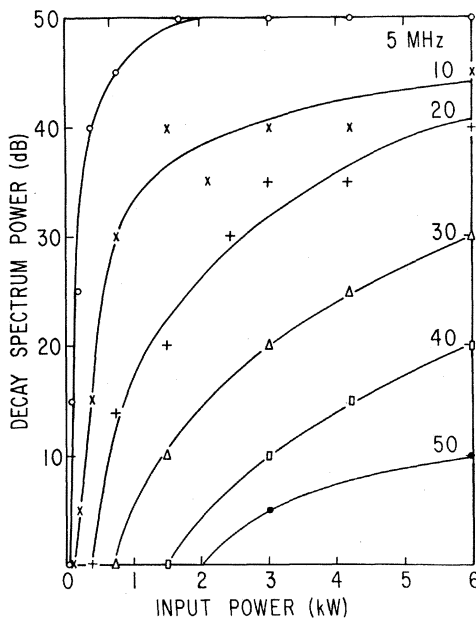


FIG. 2. Decay spectrum observed on an rf probe 50 cm from the source during pulsed heating experiments. The sideband spectrum is shown, with the low frequency ($f_0 - f_s$) as parameter.

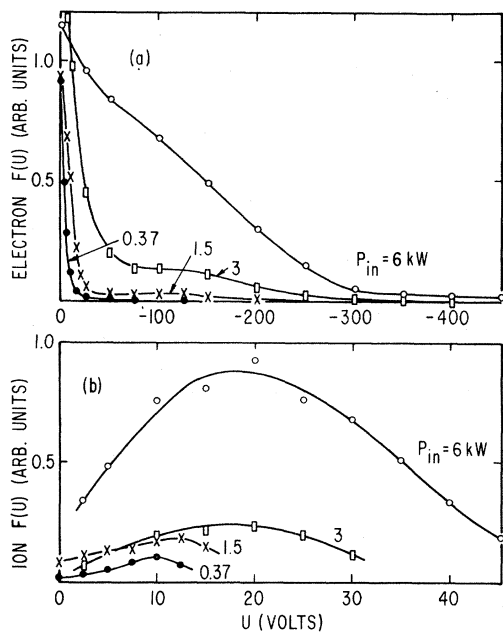


FIG. 3. (a) Electron distribution function versus energy (U). (b) Ion distribution function versus energy. $f_0/f_{ce} = 0.5$, $n_0 \approx 5 \times 10^{12} \text{ cm}^{-3}$. The input rf power, P_{in} , is the parameter.

was varied showed that at early times an energetic tail was produced, and that at later times the population of the tail was built up.

We also made a study of the heating and the decay spectrum as a function of the uniform magnetic field. We found that although the lowest thresholds occurred near $\omega_0/\omega_{ce} \approx 0.70$, the heating and the saturated spectrum level increased with increasing magnetic field. Thus, a lower

threshold did not necessarily lead to increased heating. In particular, Figs. 2 and 3 show that although the low-frequency, long-wavelength decay occurs at very low power levels (presumably due to the $\vec{j} \times \vec{B}_w$ type of decay), no substantial heating occurs until the higher-frequency, shorter-wavelength fluctuations are excited.

In conclusion, we have presented experimental results which demonstrate the fundamental aspects of the parametric and the $\vec{j} \times \vec{B}_w$ mode-mode coupling type of decay instability of large-amplitude whistler waves. The strong heating of both the electrons and the ions occurred on time scales of a few microseconds. The fast plasma heating was believed to be caused by anomalous absorption due to the short-wavelength fluctuations associated with the parametric instability.

We thank Mr. B. Grek for his help with some of the pulsed experiments and Mr. J. Johnson and J. Taylor for technical assistance.

*Work supported by the U. S. Atomic Energy Commission under Contract No. AT(11-1)-3073.

¹Y. M. Aliev, V. P. Silin, and C. Watson, Zh. Eksp. Teor. Fiz. 50, 943 (1966) [Sov. Phys. JETP 23, 626 (1966)].

²M. Porkolab, Nucl. Fusion 12, 329 (1972).

³D. W. Forslund, J. M. Kindel, and E. L. Lindman, Phys. Rev. Lett. 29, 249 (1972).

⁴G. Lisitano, M. Fontanesi, and E. Sindoni, Appl. Phys. Lett. 16, 122 (1970).

⁵G. Lisitano, M. Fontanesi, and S. Bernabei, Phys. Rev. Lett. 26, 747 (1971).

Neutron Production and Collective Ion Acceleration in a High-Current Diode*

L. P. Bradley and G. W. Kuswa

Sandia Laboratories, Albuquerque, New Mexico 87115

(Received 27 September 1972)

New measurements demonstrate that neutrons produced in a high-current pulsed diode with deuterium-bearing electrodes are of beam-target origin. During a brief portion of a 70-nsec, 2-MV, 50-kA pulse, positive ions from the anode and cathode plasmas were observed to be accelerated toward the anode rather than the cathode as dictated by the externally applied field. Energetic deuterons were observed, behind a small aperture in the anode, which were the source of neutrons produced with Li or C anodes.

The development of surface-breakdown prepulse switches has made possible the effective use of small-diameter cathodes with small anode-

cathode gap spacings on high-voltage pulsed electron accelerators. The resulting high-current densities have inspired new attempts to heat tar-

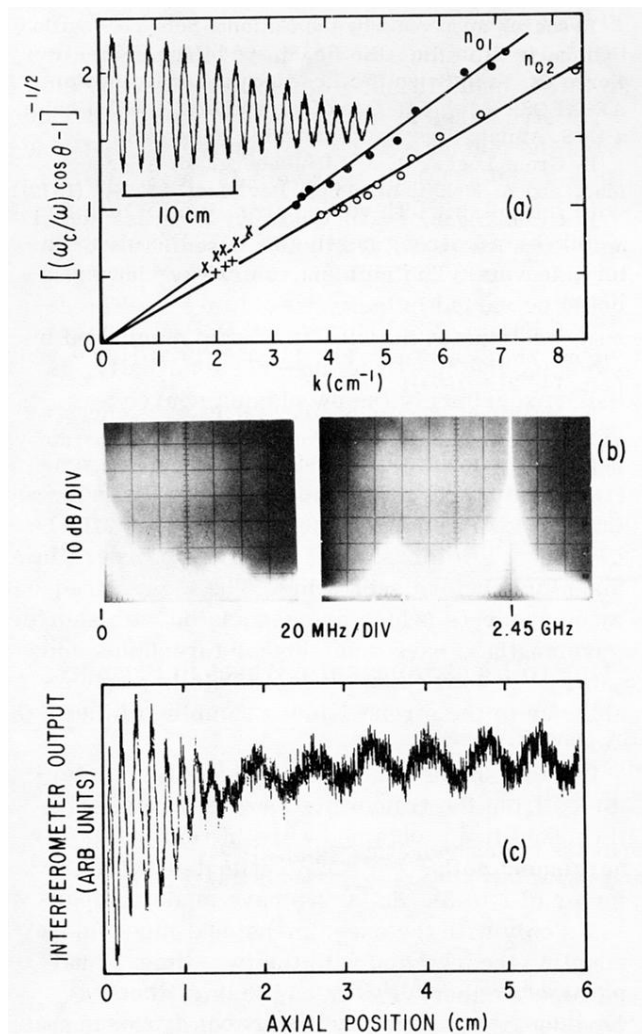


FIG. 1. (a) Experimental verification of the whistler wave dispersion relation [Eq. (2)]. The dots are associated with the rf source at 2.45 GHz. The crosses represent linearly propagated waves at 1 GHz. $n_{01} = 3.5 \times 10^{12}$, $n_{02} = 6.5 \times 10^{12}$ cm⁻³. (b) Typical decay spectrum in cw operation. $P_{in} \approx 0.8$ kW. (c) Interferometer output showing the ion acoustic waves at 7.5 MHz; $f_0/f_{ce} = 0.67$.